Infrared spectroscopy of solid CO-CO2 mixtures and layers

Broekhuizen, F.A. van; Groot, I.M.N.; Fraser, H.J.; Dishoeck, E.F. van; Schlemmer, S.

A&A 451, 723–731 (2006)
DOI: 10.1051/0004-6361:20052942

Astronomy & Astrophysics

Infrared spectroscopy of solid CO–CO_2 mixtures and layers

F. A. van Broekhuizen[1], I. M. N. Groot[1], H. J. Fraser[1,⋆], E. F. van Dishoeck[1,2], and S. Schlemmer[1]

[1] Raymond and Beverly Sackler Laboratory for Astrophysics, Leiden Observatory, PO Box 9513, 2300 RA Leiden, The Netherlands
e-mail: ewine@strw.leidenuniv.nl
[2] Leiden Observatory, PO Box 9513, 2300 RA Leiden, The Netherlands

Received 28 February 2005 / Accepted 7 November 2005

ABSTRACT

The spectra of pure, mixed and layered CO and CO_2 ices have been studied systematically under laboratory conditions using Transmission-Absorption Fourier Transform infrared spectroscopy. This work provides improved resolution spectra (0.5 cm^{-1}) of the CO_2 bending and asymmetric stretching mode, as well as the CO stretching mode, extending the existing Leiden database[a] of laboratory spectra to match the spectral resolution reached by modern telescopes and to support the interpretation of the most recent data from the Spitzer Space Telescope. It is shown that mixed and layered CO and CO_2 ices exhibit very different spectral characteristics, which depend critically on thermal annealing and can be used to distinguish between mixed, layered and thermally annealed CO−CO_2 ices. CO only affects the CO_2 bending mode spectra in mixed ices below 50 K under the current experimental conditions, where it exhibits a single asymmetric band profile in intimate mixtures. In all other ice morphologies the CO_2 bending mode shows a double peaked profile, similar to that observed for pure solid CO_2. Conversely, CO_2 induces a blue-shift in the peak-position of the CO stretching vibration, to a maximum of 2142 cm^{-1} in mixed ices, and 2140–2146 cm^{-1} in layered ices. As such, the CO_2 bending mode puts clear constraints on the ice morphology below 50 K, whereas beyond this temperature the CO_2 stretching vibration can distinguish between initially mixed and layered ices. This is illustrated for the low-mass young stellar object HH 46, where the laboratory spectra are used to analyse the observed CO and CO_2 band profiles and try to constrain the formation scenarios of CO_2.

Key words. astrochemistry – molecular data – methods: laboratory

1. Introduction

CO_2 is one of the most abundant components of interstellar ice after H_2O and CO (Gibb et al. 2004; Boogert et al. 2004; Nummelin et al. 2001; Gerakines et al. 1999; Whittet et al. 1998) and has been observed in the solid-state on lines-of-sight towards a variety of high- and low-mass stars, field stars and galactic centre sources. Surprisingly little variation in abundance exists between these objects, generally ranging from 10 to 23% with respect to H_2O-ice, although values of 34 to 37% have been reached for some low- and intermediate mass sources (Nummelin et al. 2001; Boogert et al. 2004; Pontoppidan et al. 2005). In the gas phase, observations imply that the CO_2 abundance is a factor of ∼100 less than in the solid state (van Dishoeck et al. 1996; Boonman et al. 2003), indicating that CO_2 forms in the solid-phase. The most popular formation mechanism is via energetically mediated reactions such as UV photolysis of mixed H_2O−CO ices (Watanabe & Kouchi 2002). However, the fact that CO_2 ice is also observed towards the quiescent clouds in front of Elias 16, where there is little if any UV-induced chemistry, suggests that no energetic ice-processing is required for CO_2 formation, so surface reactions involving CO must play a key role (Whittet et al. 1998; Roser et al. 2001). Whichever formation route is invoked, a direct link is implied between the location of CO and CO_2 within interstellar ices.

Recent high resolution observations of solid CO towards a large sample of embedded objects using the VLT-ISAAC spectrometer show that 60−90% of solid CO in interstellar ices resides in a nearly pure form, and that a significant number of the sources show evidence for CO in a H_2O-rich environment, at a minimum abundance of 19% with respect to the pure CO component (Pontoppidan et al. 2003; Boogert et al. 2004; Fraser et al. 2004). Given these constraints, CO_2 may form via surface reactions on the pure CO-ice layer, resulting in a bi-layered ice-structure. Alternatively, if CO_2 forms from UV- and cosmic ray-induced reactions involving CO in the H_2O-rich environment, one can envisage that CO_2 will reside in a H_2O-rich ice without being in direct contact with CO. The latter situation has been simulated in detail in the laboratory by, for example, Gerakines et al. (1995) and Ehrenfreund et al. (1999), who recorded infrared (IR) spectra of mixed ices.

The key aim of this paper is to establish the influence CO may have on the CO_2 spectral features and vice versa. In addition to the spectroscopic features of CO at 2139 and

⋆ *Current adress*: Department of Physics, University of Strathclyde, John Anderson Building 107 Rottenrow, Glasgow G4 0NG, Scotland.
[a] http://www.strw.leidenuniv.nl/~lab/databases/

2136 cm^{-1} in pure and H_2O-rich ice environments respectively, a third component of the interstellar CO-ice band has been detected at around 2143 cm^{-1} along many lines of sight. In the VLT-ISAAC and other surveys, this band was attributed to the TO-component of the pure CO ice feature, which under certain conditions is split into two sharp features (Collings et al. 2003a; Pontoppidan et al. 2003). However, Boogert et al. (2002) assign this band to CO in a CO_2 dominated environment. This paper therefore also analyses the presence or absence of the 2143 cm^{-1} feature in the spectra of CO−CO_2 laboratory ices, as a function of the morphology (i.e., the configuration of CO and CO_2 in the CO−CO_2 ice system: either mixed or separated in two spatially distinct layers) and temperature, to find the origin of this band.

Solid CO_2 can be observed in interstellar spectra by its 4.3 μm asymmetric stretching (ν_3) and 15 μm bending (ν_2) modes. The ν_2 mode is known to be very sensitive to the local ice environment but is weaker than the stretching mode. The higher sensitivity of the recently launched Spitzer Space Telescope, compared to that of its predecessor the Infrared Space Observatory (ISO), has made it possible to conduct a detailed analysis of the $\nu_2(CO_2)$ band over a wider range of interstellar objects. First results show that the CO_2 abundances are similar to or higher than those deduced with ISO (Watson et al. 2004; Boogert et al. 2004; Pontoppidan et al. 2005). Thus, there is the possibility to combine the new observational data of solid CO_2 with VLT observations of CO to place constraints on the CO_2 ice environment.

Previous laboratory studies have dealt with mixtures of binary ices composed of CO and CO_2 (Ehrenfreund et al. 1996, 1997; Elsila et al. 1997). These proved very useful for interpreting interstellar ice observations. However, more systematic studies including layered ices are necessary to link the spectral characteristics to the interstellar environments mentioned above. This work therefore presents the effects of CO on the spectroscopy of the CO_2-bending and stretching modes as well as the influence of thermal annealing in pure, mixed and layered ice systems. The data are taken at an increased spectral resolution of 0.5 cm^{-1} with respect to the previous laboratory studies, in order to resolve the CO_2-bending mode and the CO-stretching vibration and meet the accuracy of the VLT-ISAAC and Spitzer data as well as future mid-infrared spectra to be obtained with the James Webb Space Telescope. The experimental details are explained in Sect. 2. The spectroscopic behaviour of CO and CO_2 are presented and discussed in Sects. 3 and 4, respectively, as a function of the temperature and ice composition. In Sect. 5 the astrophysical implications are discussed and one example of a comparison between the new experimental data with observations is given.

2. Experimental procedure

All experiments were conducted in a high vacuum (HV) chamber described in detail elsewhere (Gerakines et al. 1995), at a base-pressure below 2×10^{-7} Torr. Ices of $^{12}C^{16}O$ (Praxair 99.997% purity) and $^{12}C^{16}O_2$ (Praxair 99.997% purity) were grown on the surface of a CsI window, pre-cooled to 15 K, via effusive dosing at a growth rate of $\sim 10^{16}$ molec $cm^{-2}\,s^{-1}$, directed at 45 degrees to the surface normal. Transmission Fourier Transform Infrared spectra of the ice systems were recorded at 0.5 cm^{-1} resolution at fixed temperatures between 15 to 100 K, using a total of 128 scans between 4000−400 cm^{-1} and a zero filling factor of 4. Each recording lasted 20 min, and was started directly after the temperature had equilibrated, which took 2 min.

The pure and layered ice structures were grown in situ, via single and sequential dosing from CO and CO_2 gas bulbs, filled to a total pressure of 10 mbar, prepared on a separate glass vacuum manifold, with a base-pressure of $\sim 10^{-5}$ mbar. Mixed ices were prepared by dosing gas from pre-mixed CO and CO_2 bulbs.

The Full Width at Half Maximum (*FWHM*) and peak-position of the CO-stretching, CO_2-bending and CO_2 asymmetric stretching mode were determined using the Levenberg-Marquardt non-linear least square fitting routine within Origin 7.0. Uncertainties in the peak-centre position and *FWHM* were typically less than 0.05 cm^{-1}, except close to the desorption temperature where uncertainties may be larger.

Previous work on the spectroscopy of CO_2-ice has indicated that the ice structure (i.e. amorphous or crystalline) influences its spectral profile (Falck 1986), although some uncertainty exists as to the extent of the crystallinity of low temperature vapour deposited CO_2-ice (Falck 1986; Sandford et al. 1988; Sandford & Allamandola 1990). Consequently, optical constants have not been derived for the ices studied here. Before doing so, a systematic study is required of the degree of crystallinity in pure, vapor-deposited CO_2 ices and the influence of these phases on the CO_2 spectroscopy, which will be the topic of future work.

The range of ices studied here are summarised in Table 1. The relative concentrations of CO and CO_2 range from 0.1 to 2 CO/CO_2, relevant for comparison with observations of high- and low-mass YSO's, which show CO/CO_2 column density ratios of 0.1−1.3 (Gibb et al. 2004). All of the raw laboratory spectra discussed here have been made available through the Internet at `http://www.strw.leidenuniv.nl/~lab/mixed_layered_CO_CO2/`.

3. Results

3.1. CO_2-bending mode

Figure 1 shows the spectra of $\nu_2(CO_2)$ at 15 K in pure and some example mixed and layered ices (with CO), together with the thermal evolution of each band. In the pure ice (Fig. 1a), the ν_2 spectrum at 15 K has two components, peaking at 654.7 and 659.8 cm^{-1} (marked by grey lines) with *FWHM* of 1.8 and 3.1 cm^{-1}, respectively, showing a Davidov splitting due to a highly ordered ice structure (e.g., Decius & Hexter 1977; Sandford & Allamandola 1990). This profile changes gradually beyond 40 K as both peak intensities increase while their *FWHM* decrease until the point at which CO_2 desorbs, in agreement with previous findings of Sandford & Allamandola (1990). The integrated area is observed to increase with temperature, but by no more than 20%. This increase is consistently found in the bending mode spectra during the warm-up

Table 1. Ice compositions.

Ice morphologies	Nomenclature	Conc. ratio CO	Conc. ratio CO_2	Exposure (s)	Approx. ice [a] thickness (L)
pure	CO	1	–	60	600
	CO_2	–	1	60	600
layered	1/1 CO/CO_2	1	1	60 + 60	1200
	1/1 CO_2/CO	1	1	60 + 60	1200
	1/2 CO/CO_2	1	2	60 + 120	1800
	2/1 CO_2/CO	2	1	120 + 60	1800
	3/1 CO_2/CO	3	1	180 + 60	2400
	10/1 CO_2/CO	10	1	600 + 60	6600
mixed	1:1 CO:CO_2	1	1	120	1200
	2:1 CO:CO_2	2	1	180	1800
	1:10 CO:CO_2	1	10	660	6600

The nomenclature adopted uses *A*:*B* to denote mixtures and *A*/*B* to indicate layered structures with *A* on top of *B*. [a] 1 L = 10^{15} molec cm^{-2} ≈ 1 mono-layer.

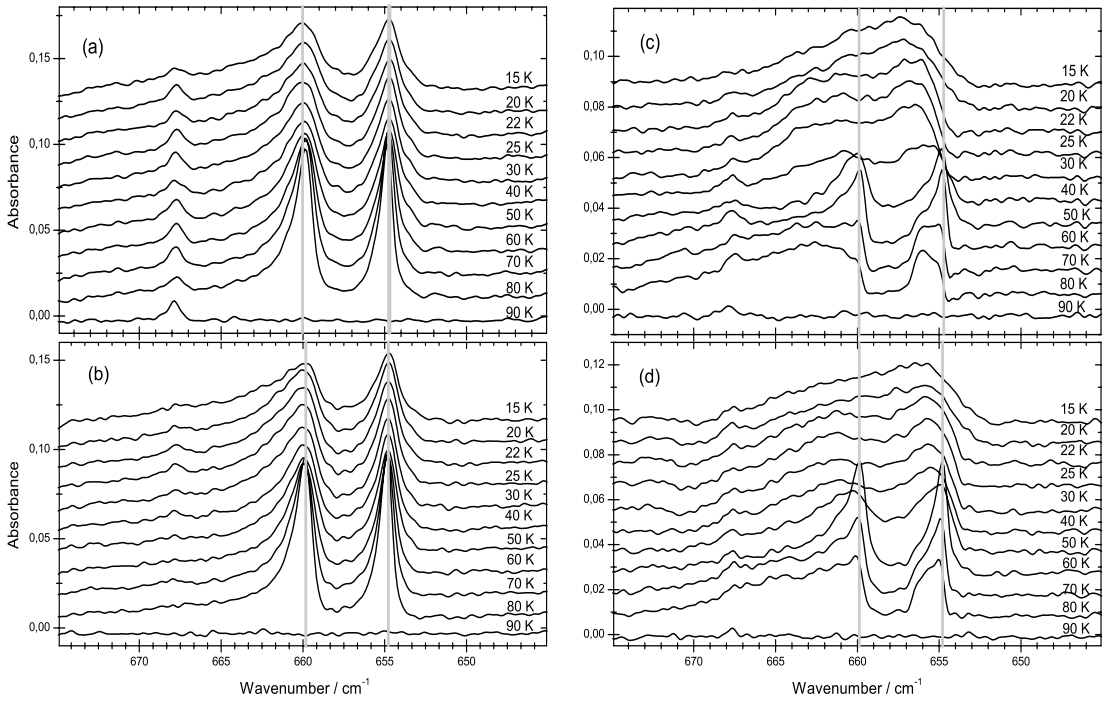

Fig. 1. The thermal evolution of the CO_2-bending mode for **a)** pure CO_2-ice; **b)** a 1/1 CO/CO_2 layered ice; **c)** 2:1 CO:CO_2; and **d)** 1:1 CO:CO_2 ice mixtures, from 15–90 K. The two vertical grey lines mark the positions of the two peaks of the bending mode at 15 K in pure CO_2-ice.

of pure and layered ices. This is in contrast with the spectral behaviour of the CO_2 stretching mode (see Sect. 3.2), which does not show any increase in integrated band strength but stays constant within 5%. The spectral profile and thermal behaviour is very similar in 1/1 CO/CO_2, shown in Fig. 1b. Interestingly, this appears to be independent of whether CO_2 is deposited on top or underneath the CO-ice layer (data not shown).

Conversely, when CO_2 is mixed with CO, the ν_2 spectrum changes drastically (see also Ehrenfreund et al. 1997; Elsila et al. 1997). At 15 K, the 2:1 and 1:1 CO:CO_2 ices, Figs. 1c and 1d respectively, show one broad asymmetric band without any sub-structure, peaking at between 655 and 657 cm^{-1}. However, from the present experiments it is clear that at 22 K, some sub-structure becomes visible, which evolves to a doublet beyond 40 K. This doublet is similar to that of pure CO_2-ice, but the peaks remain slightly broader and more asymmetric. Under the present experimental conditions, CO_2 desorbs between 80 and 90 K in all the ices studied. The exception is 1:10 CO:CO_2. Its 15 K spectrum exhibits two peaks centred at 654.7 and 659.8 cm^{-1} (*FWHM* of 3.6 and 6.1 cm^{-1}) and its thermal behaviour is similar to that of pure CO_2-ice. However, its desorption is retarded to 90–100 K.

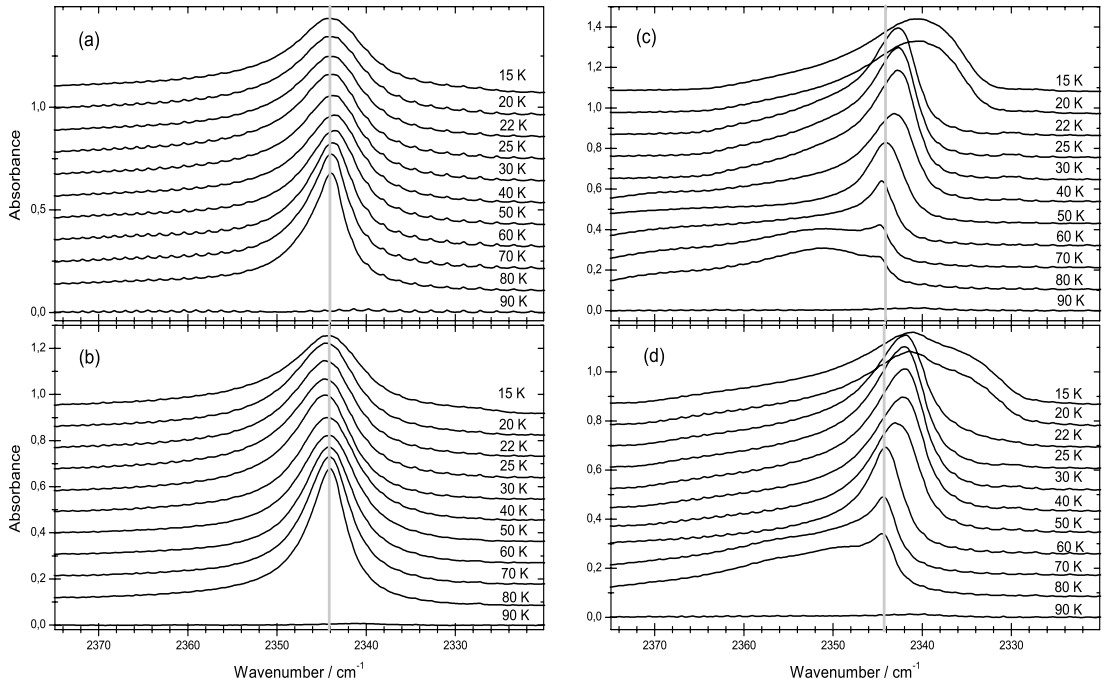

Fig. 2. The thermal evolution of the asymmetric stretching mode of CO_2 in **a)** pure; **b)** 1/1 CO/CO_2; **c)** 2:1 CO:CO_2; and **d)** 1:1 CO:CO_2, from 15–90 K. The grey line marks the peak-centre position at 15 K in pure CO_2-ice.

A small artifact is occasionally evident in Fig. 1 at 667.8 cm^{-1}, which is clearly not associated with CO or CO_2 since it remains in the spectra after CO_2 desorbs.

3.2. CO_2 asymmetric stretching vibration

Figure 2 shows the thermal evolution of the $\nu_3(CO_2)$ for the same four ices as Fig. 1. As with the ν_2 mode, the trend observed is that almost no spectral differences are seen between the pure and layered ices (Figs. 2a and 2b), whereas peak-position and *FWHM* differences are observed between the pure and the mixed ices (Figs. 2a and c−d). This indicates that it will be difficult to distinguish between pure and layered ices in interstellar spectra. However, since the thermal evolution of mixed and layered ices are different, the comparison between these two cases can help to unravel the environmental history of interstellar ices.

In pure CO_2-ices at 15 K, the $\nu_3(CO_2)$ band peaks at 2344.0 cm^{-1} (*FWHM* of 10.6 cm^{-1}), independent of temperature. Its *FWHM*, however, starts to decrease gradually beyond 40 K as the peak intensity increases until CO_2 desorbs. In mixtures (Figs. 2c and 2d, respectively) at least three different spectral components are visible due to the higher resolution used compared to previous studies (e.g., Sandford & Allamandola 1990; Ehrenfreund et al. 1997). At 15 K, the spectral profile is dominated by a broad asymmetric band, peaking at 2339.9 cm^{-1} (*FWHM* of 13.3 cm^{-1}), which exhibits a shoulder at around 2334 cm^{-1} in the case of 1:1 CO:CO_2. By 22 K, the spectrum has evolved into a pure ice like feature, peaking at 2342.5 cm^{-1}, which beyond 50 K shows the development of a third component at around 2351 cm^{-1}.

3.3. CO-stretching vibration

Figure 3 shows the thermal behaviour of the CO-stretching mode for the same four ices as Fig. 1. The spectrum of pure CO-ice (Fig. 3a) peaks at 2138.7 cm^{-1} (*FWHM* of 1.6 cm^{-1}) and is independent of temperature. This differs from the results of Sandford et al. (1988) who observed a band narrowing with increasing temperature. A shoulder, visible at ∼2141 cm^{-1} (black arrow), was observed previously by Sandford et al. (1988) and is discussed in the context of CO trapping in ices by Fraser et al. (in prep., hereafter FR06a). Under the present experimental conditions, pure CO desorbs between 25−30 K.

Again, the CO spectra of layered ices are almost identical to that of pure CO ice. However, beyond 22 K in 1/1 CO/CO_2 (Fig. 3b), the 2141 cm^{-1} shoulder gets relatively more pronounced. This effect becomes stronger with increasing thickness of the CO_2 layer and is best seen in Fig. 4 for the most extreme case of CO_2/CO studied here, 10/1. There, the intensity of the main peak (2138.9 cm^{-1}) clearly decreases from 22 to 30 K while the "shoulder" at 2141 cm^{-1} becomes more intense and a third feature appears at around 2145.5 cm^{-1} (both indicated by an arrow). These new features start decreasing in intensity when CO desorbs from 30 K onwards. However, because the 2141 cm^{-1} feature reduces faster, this leads to a blue-shift of the overall CO band. From 40–60 K, also the 2145.5 cm^{-1} environment is lost, which shifts the overall band position back to the red before the remaining CO finally desorbs (with the CO_2) above 80 K.

All mixed ices (Figs. 3c and 3d) show broadened and blue-shifted spectra compared to the pure case, centred between 2140.3 and 2141.6 cm^{-1}, with *FWHM* extending from 5.6 to 9.0 cm^{-1} (see also Elsila et al. 1997). Equimolar mixtures induce the strongest blue-shifts. Thermal warming

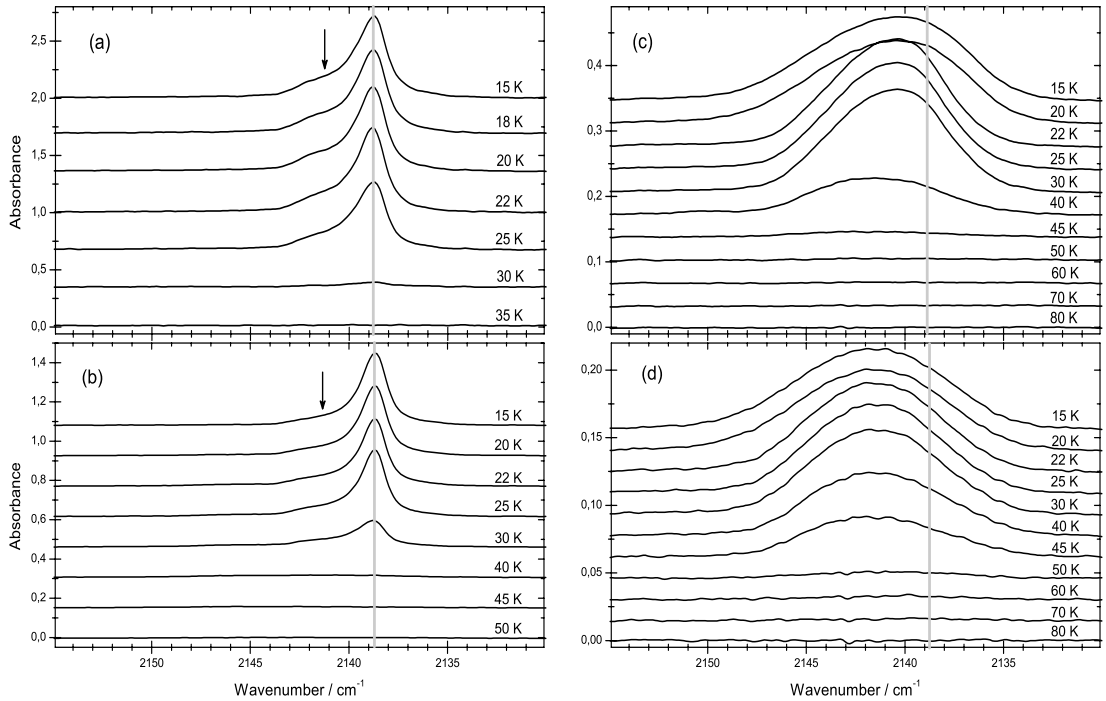

Fig. 3. The thermal evolution of the CO-stretching vibration in **a)** pure CO-ice; **b)** 1/1 CO/CO_2; **c)** 2:1 CO:CO_2; and **d)** 1:1 CO:CO_2 from 15–80 K. The grey line marks the position of the main peak at 15 K in pure CO-ice.

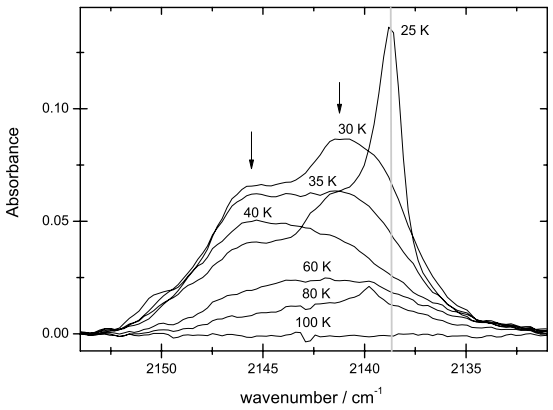

Fig. 4. The thermal evolution of the CO-stretching vibration in a 10/1 CO_2/CO layered ice system, from 25–100 K. The thick grey line line marks the peak-centre position of the main spectral feature in pure CO-ice at 15 K. The two arrows indicate the two shoulders that evolve as the temperature increases.

only narrows the band between 20 and 22 K to a *FWHM* between 6.5 and 7.6 cm^{-1} (broader than predicted by Ehrenfreund et al. 1997). CO desorption starts around 30 K and continues up to 50–60 K in 2:1 and 1:1 CO:CO_2, or 90−100 K in the case of 1:10 CO:CO_2 (not shown). None of the data show evidence for an isolated CO-feature centred at 2143 cm^{-1}, as suggested for CO−CO_2 interactions in interstellar ices by Boogert et al. (2002).

4. Discussion

The results described in Sect. 3 provide clear evidence that the morphology of CO- and CO_2-containing ices affects their spectroscopy. The peak positions and *FWHM* of all ices studied are summarised in Figs. 5 (CO_2-bending mode) and 6 (CO-stretching mode) to simplify the evaluation of the spectral changes as functions of temperature and ice morphology. For a similar evaluation of the CO_2-stretching mode, see Appendix A in the online article. The associated uncertainties of these data have been calculated (see Sect. 2) but error bars are omitted from the plots for clarity. The actual ice structure and the physical processes that give rise to these spectra are discussed by Fraser et al. (in prep., hereafter FR06b).

In Figs. 5 and 6, the thermally induced spectroscopic changes appear at 22, 30 and 50 K, related to CO bulk-diffusion, the onset of CO desorption from pure CO ice and the temperature at which pure CO_2 ice undergoes major restructuring, respectively (see for further discussion Collings et al. 2003b, FR06a and FR06b).

It is clear from Figs. 5a–c that the $\nu_2(CO_2)$ spectrum is always split into two fully resolved peaks where CO_2 dominates the ice matrix, i.e. in pure and layered ices, in (close to) equimolar mixed ices at $T > 50$ K, and in very dilute CO mixtures (i.e. 1:10 CO:CO_2). Despite the very similar band profile of the $\nu_2(CO_2)$ in all ices beyond 50 K, the $\nu_3(CO_2)$ spectra (see Fig. 2 and Appendix A) indicate that the line profiles of the vibrational spectra in pure, layered and mixed CO:CO_2 ices are distinct from each other, suggesting that each ice morphology evolves a distinct structure on annealing. This shows the importance of observing both the bending and stretching mode vibrations of CO_2, to be able to constrain the interstellar ice environment of CO_2 and its history.

Figure 6 shows the main positions and *FWHM* of the CO-stretching mode. The temperature-independent band position of CO in mixtures (Fig. 6c) is consistent with the fact

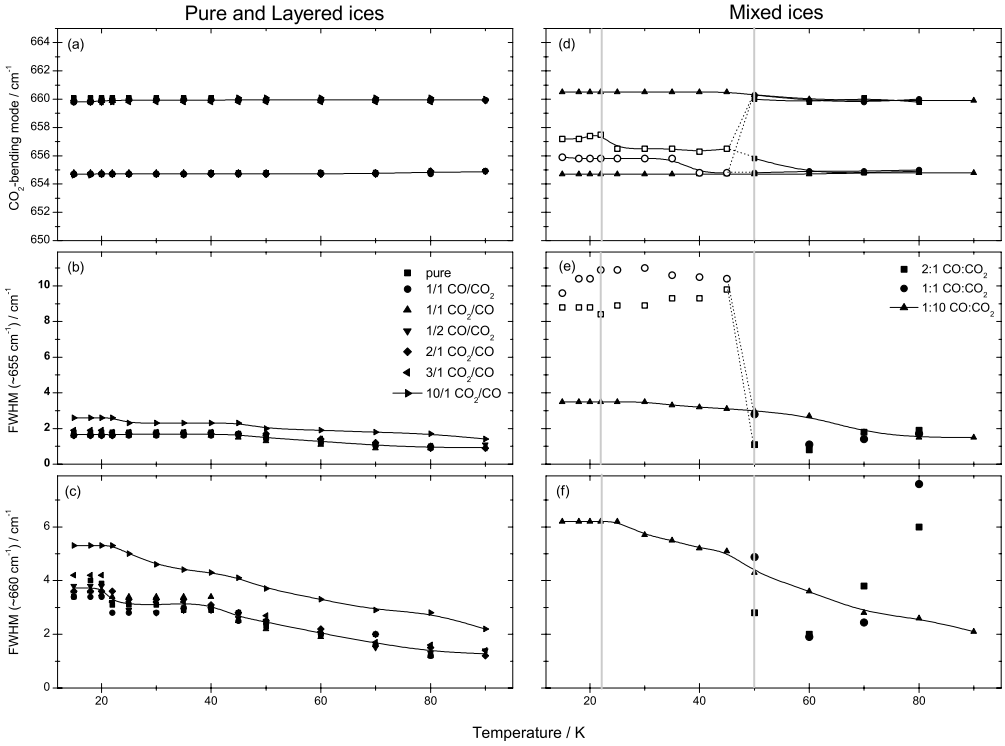

Fig. 5. The peak-centre positions and *FWHM* of the main spectral features of the CO_2-bending mode, plotted as a function of ice temperature. **a)** Peak-centre positions in the pure and layered ices with the corresponding *FWHM* of the feature centred at **b)** 655 cm^{-1}; and **c)** 660 cm^{-1}. **d)** Peak-centre positions in the mixed ices with the corresponding *FWHM* of the peak at **e)** 655 cm^{-1}; and **f)** at 660 cm^{-1}. The legend in **b)** gives the symbol assignment for all three left-hand panels, that in **e)** for all three right-hand panels. Open symbols indicate the presence of only a single peak, whereas solid symbols mark the presence of the doublet. In each of the panels, spline-fits through the data points guide the eye, except in **e)** and **f)** where beyond 50 K peak positions and *FWHM* are more difficult to assign. The two vertical grey lines enclose the temperature range between 22 and 50 K (see text for details).

that CO likely remains bound in the CO_2 matrix over the full temperature range, implying the absence of ice segregation. In layered ices, the fraction of CO that remains trapped or bound somehow in the CO_2 layer exhibits spectra that are similar to those of mixtures, both in peak position and in *FWHM*. This suggest that layered ices are thermally mixing. This "mixing" apparently does not affect the CO_2 ice structure since the $\nu_2(CO_2)$ spectra (Figs. 5b–c) show no detectable peak broadening.

The horizontal lines in Fig. 6 indicate the positions and *FWHM* of the three phenomenological interstellar CO-ice components (Pontoppidan et al. 2003). The red component (rc) is associated with a CO–H_2O environment and will not be further addressed here. The middle component (mc), associated with pure CO-ice, lies close to the peak-centre position of the CO spectrum in pure and layered laboratory ices. The blue component (bc) has been invoked as being indicative of CO:CO_2 mixtures in interstellar ice. However, no direct match is found between the position of this bc and the band positions of the ices studied here, although both mixed and layered ices do contain a blue spectral wing. Also, Figs. 6b and 6d show that all ice components between 2141−2146 cm^{-1} have *FWHM* 1.5 to 3 times larger than that of the bc. Such evidence does question the assignment of a 2143 cm^{-1} feature to CO:CO_2 ices but cannot rule it out completely. Further work will be required on LO-TO splitting of the CO-stretching mode (a plausible alternative carrier of the 2143 cm^{-1} feature, see Collings et al. 2003a) on this same subset of ice morphologies in the laboratory. A detailed analysis of high *S/N* interstellar line profiles is needed of sources that exhibit a strongly pronounced CO blue wing (e.g., L 1489, SVS 4−9, Reipurth 50 and RNO 91, Pontoppidan et al. 2003) and a single-peaked CO_2 bending mode profile before the assignment of the CO 2143 cm^{-1} band can be fully resolved.

5. Astrophysical implications

The power of combining CO- and CO_2-observational data to elucidate the local environment of both molecules in interstellar ices is illustrated here for the low-mass object HH 46. Its $\nu_2(CO_2)$ and CO-stretching mode were recently studied in detail by Boogert et al. (2004). Here, these bands are reanalysed to establish the maximum possible contribution from a CO−CO_2 ice component.

Figure 7(I, left) shows the $\nu_2(CO_2)$ spectrum observed with Spitzer (solid black line; CO_2 stretching mode not observed, Boogert et al. 2004). The substructure at ~658 cm^{-1} (15.2 μm) shows a weak doublet profile, but the peaks of the doublet are not narrow enough to originate from the $\nu_2(CO_2)$ band of pure CO_2 ice ($T \geq 10$ K). Instead, the more broad profile of the $\nu_2(CO_2)$ laboratory spectrum that arises when CO_2 is mixed in CO at elevated temperatures provides a much

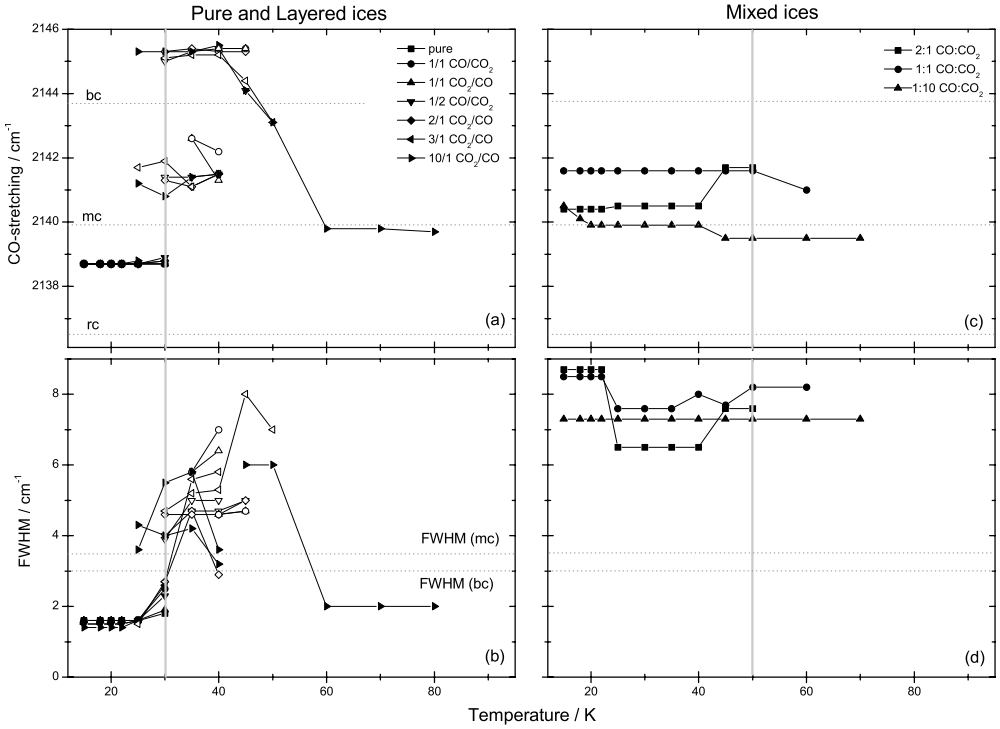

Fig. 6. The main peak-centre positions and *FWHM* of the CO-stretching vibration, plotted as a function of ice temperature. **a)** Peak-centre positions in pure and layered ices with **b)** their corresponding *FWHM*. **c)** Peak-centre positions in mixed ices with **d)** their corresponding *FWHM*. The legend in **a)** gives the symbol assignment for the two left-hand panels, that in **c)** for the right-hand panels. Solid symbols indicate strong bands ($S/N > 5$); open symbols indicate very weak bands, S/N 1−2 at best. Symbols indicating the same feature are connected by lines to guide the eye. The vertical grey line in the left panels marks the temperature at which pure CO desorbs, that in the right panels marks the temperature at which the single peak profile of the CO_2-bending mode in a mixture converts to a doublet. The three horizontal (dotted) lines in **a)** and **c)** indicate the line centres of the three components of the phenomenological fit to the interstellar solid CO-band observed by Pontoppidan et al. (2003; see text). The two dotted lines in **b)** and **d)** give the *FWHM* of the mc and rc of the fitted components. It should be noted that the *FWHM* and peak positions of laboratory spectra can be altered due to grain shape effects.

better match. Therefore, in Fig. 7(I) the $\nu_2(CO_2)$ of HH 46 is matched by combining the laboratory spectrum of $\nu_2(CO_2)$ of 2:1 CO:CO_2 ice at 40 K (dotted line) and one at 10 K in a 10:1 H_2O:CO_2 mixed ice (similar to that of Boogert et al. 2004, light grey dashed line). Grain shape effects may affect the interstellar profile of the first spectrum, although the ice is no longer a homogeneous mixture (FR06b). Since no optical constants are available, these effects are not taking into account. The overall match (grey line) reproduces the observed band profile, although the small feature at 662 cm^{-1} and the red-wing beyond 650 cm^{-1} are less well matched than by Boogert et al. (2004). The results are listed in Table 2. As can be seen from Table 2, only 4% of all CO_2 is present in the CO ice (an abundance of 1.3% with respect to H_2O). The majority of the CO_2 (96%) appears to be mixed with the H_2O ice. Obviously, this mix and match procedure can only provide a rough estimate of the (maximum) column density of the CO−CO_2 ice component contributing to the CO_2-bending mode and is only meant to illustrate how laboratory data of binary ices of CO and CO_2 can constrain the interstellar ice environment of CO_2.

Figure 7(II, right) shows the spectrum of the solid CO-stretching mode observed (solid line) by VLT-ISAAC Pontoppidan et al. (2003). Using the same laboratory spectrum (2:1 CO:CO_2 at 40 K, thick solid line in Fig. 7(IIa)) to fit the blue wing of the CO ice, adding in a 1:10 CO:H_2O ice at 10 K (dashed line) and a pure CO ice component (the mc of interstellar CO-ice, dotted line), gives an abundance of CO in CO:CO_2 of 2.1% with respect to H_2O ($\chi^2 = 1.3$; see Table 7). This is 11% of the total CO present. The results in Fig. 7(I) and (IIa) show that the interstellar CO and $\nu_2(CO_2)$ bands of HH 46 can be fit consistently with spectra of a single 2:1 CO:CO_2 laboratory ice mixture. In comparison the purely phenomenological fit of the CO band in Fig. 7(IIb) ($\chi^2 = 1.2$) gives a bc (representing the CO:CO_2 ice or possibly the LO-TO splitting of pure CO ice; see also Sect. 4), which is a smaller fraction of the total CO abundance, only 5% (see Table 7). Further analysis of a much larger sample of sources is needed to distinguish between these cases and find systematic trends with other parameters such as temperature. Such systematic studies can then address the different formation scenarios of CO_2 in the presence of CO and/or H_2O described in Sect. 1, in particular whether the amount of CO_2 formed with CO is generally only a small fraction of the total CO_2, as found for HH 46.

6. Conclusion

In summary, the experimental work presented here shows that CO only affects the CO_2-bending mode in intimate mixtures

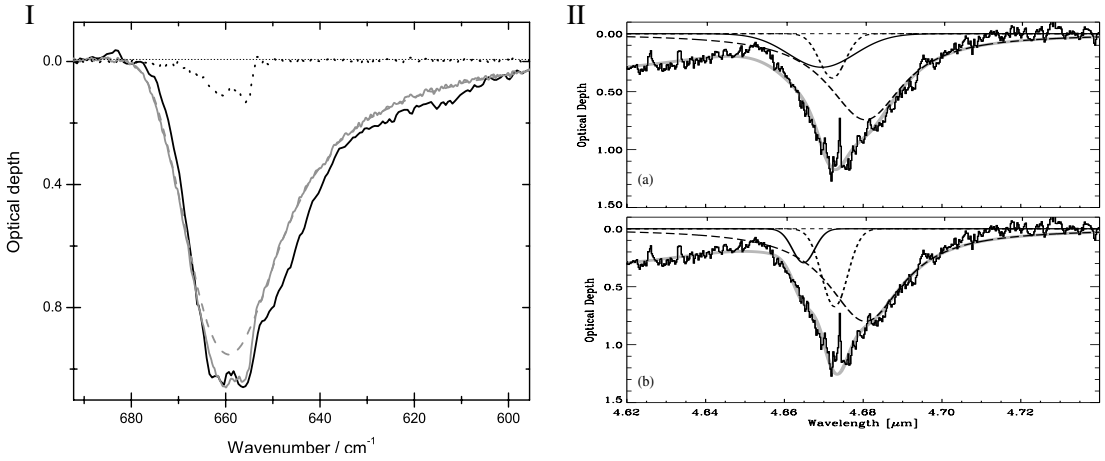

Fig. 7. *I, Left*: the $\nu_2(CO_2)$ as observed toward HH 46 by Spitzer (black solid line, Boogert et al. 2004), reproduced by a combination of a laboratory spectrum of 10:1 H_2O:CO_2 at 10 K (light grey dashed line) and a 2:1 CO:CO_2 at 40 K (dotted line). The resulting match is shown by the dark grey line. *II, Right*: the CO-stretching mode as observed towards HH 46 by VLT-ISAAC (solid line). Two different fits are shown, adopting **IIa)** the laboratory spectrum of 2:1 CO:CO_2 at 40 K (thick solid line) and of 1:10 CO:H_2O at 10 K (dashed line), and the mc of solid CO (dotted line), and **IIb)** the bc, mc, and rc component of solid CO (Boogert et al. 2004). In both plots, the total fit to the CO band is shown in grey, including a Gaussian fit to the XCN band to the blue of the CO stretching mode.

Table 2. Results of the CO−CO_2 fit toward HH 46.

Ice component	N (10^{17}) [a] molec cm^{-2}	$N/N(CO_2)_{tot}$	$N/N(CO)_{tot}$	$N/N(H_2O)$ [b]
$(CO_2)_{tot}$	26 [c]			0.335
CO_2 (in CO)	1.0 [d]	0.04		0.013
$(CO)_{tot}$	16 [c]			0.195
CO (in CO_2)	1.7 [e]		0.11	0.021
CO (bc)	0.8 [f]		0.05	0.010

Maximum amounts in CO:CO_2 mixtures consistent with data. [a] $A_{\nu_2(CO_2)} = A_{CO} = 1.1 \times 10^{-17}$ cm molec^{-1} (Gerakines et al. 1995). [b] $N(H_2O) = 8.0 \times 10^{18}$ cm^{-2} (Boogert et al. 2004). [c] From Boogert et al. (2004). [d] Integrated area of CO_2 bending mode spectrum at 40 K in 2:1 CO:CO_2 is 1.10 cm^{-1}. [e] $\tau_{4.67\,\mu m} = 0.27 \pm 0.01$, *FWHM* of 7 cm^{-1}. [f] $\tau_{bc} = 0.30 \pm 0.01$, *FWHM* of 3.0 cm^{-1}.

below 50 K (under the present experimental conditions), where mixing of CO and CO_2 results in a single asymmetric band profile for the CO_2 bending mode. In all other CO−CO_2 ice morphologies studied here the CO_2-bending mode shows the same doublet profile. Conversely, the CO-stretching vibration is blue-shifted to a maximum of 2142 cm^{-1} in intimate mixtures with CO_2 and between 2140 and 2146 cm^{-1} when CO interacts with a layer of initially pure CO_2. The assignment of an interstellar "2143 cm^{-1} feature" by CO in layered ices with CO_2, however, is difficult. Further constraints on its assignment require (at least) the analysis of the interstellar CO_2 bending- and future observations of CO_2 stretching mode spectra. The laboratory data do indicate that the combined band profiles of CO and CO_2 can be used to distinguish between mixed, layered and thermally annealed CO−CO_2 ices. Ultimately, this can provide important constraints on the formation mechanism of CO_2, one of the most abundant interstellar ices.

Acknowledgements. This research was financially supported by the Netherlands Research School for Astronomy (NOVA) and a NWO Spinoza grant. The authors would like to thank Klaus Pontoppidan for helpful discussions and Adwin Boogert for kindly providing the Spitzer CO_2 data of HH 46.

Appendix A: CO_2 asymmetric stretching mode

In analogy to Figs. 5 and 6, the peak position and *FWHM* of all ices studied are summarised in Fig. A.1 for the CO_2 asymmetric stretching mode. Section 3.2 describes in detail that the spectral profile of the CO_2 asymmetric stretching mode and its temperature dependence are very similar for pure and layered ices with CO, but are significantly different compared to CO:CO_2 mixtures. This is even more clear from Fig. A.1 if the right and the left hand panels are compared.

From Fig. A.1a, it is clearly seen that the peak position of the CO_2 asymmetric stretching mode does not change with increasing temperature in pure or layered ices, although its *FWHM* (Fig. A.1b) does show a small decrease. However, in mixtures the peak position shows significant shifts to higher wavenumbers and the appearance of new components as the temperature increases. This behavioural difference between mixed and layered ices with CO indicates that (future)

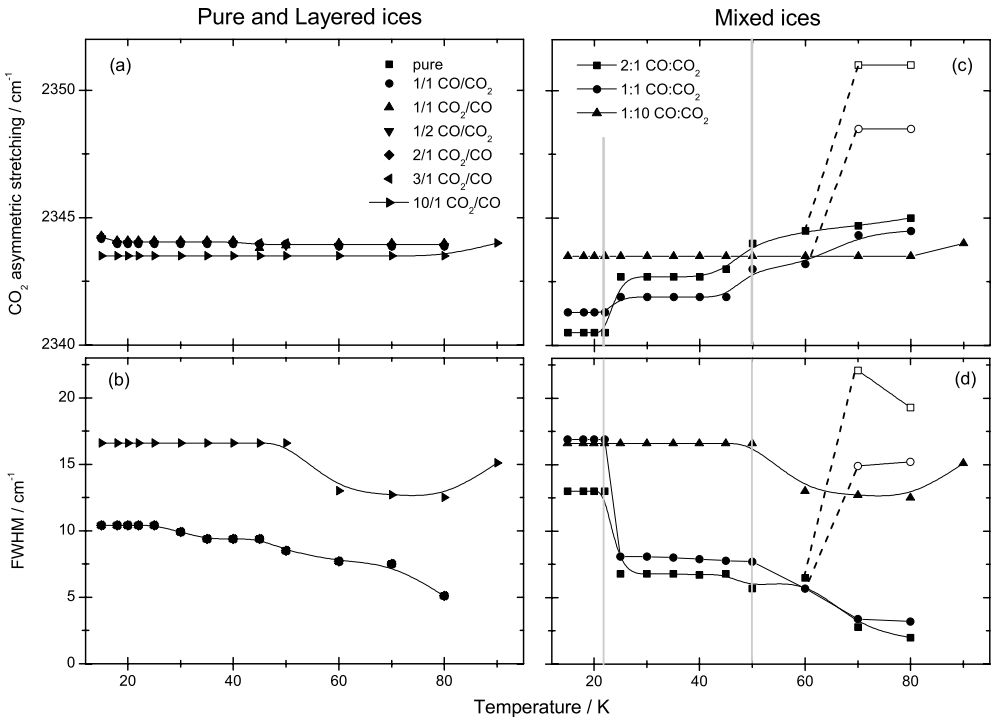

Fig. A.1. The peak-centre positions and *FWHM* of the main spectral features of the CO_2 asymmetric stretching vibration, plotted as a function of the ice temperature. **a)** Peak-centre positions in pure and layered ice with **b)** the corresponding *FWHM*. Note that most of the data points overlap in **a)** and **b)**. **c)** Peak-centre positions in mixed ices with **d)** the corresponding *FWHM*. The legend in **a)** gives the symbol assignment for the two left-hand panels, that in **c)** for the right-hand panels. Open and closed symbols are used to indicate independent peaks present at the same temperature. In each of the panels, spline-fits through the data points guide the eye. In **c)** and **d)**, the two vertical grey lines enclose the temperature range between 22 and 50 K and the dashed lines connect two separate features that appear in the same spectrum.

observations of the CO_2 asymetric stretching mode in interstellar ice spectra can provide important additional information on the interstellar ice composition and its evolutionary history. Because the CO_2 asymmetric stretching band is sensitive to the CO:CO_2 environment, spectral information of this band might also contribute to a better understanding of the nature of the bc component of interstellar CO-ice (see Sect. 4).

References

Boogert, A. C. A., Blake, G. A., & Tielens, A. G. G. M. 2002, ApJ, 577, 271

Boogert, A. C. A., Pontoppidan, K. M., Lahuis, F., et al. 2004, ApJS, 154, 359

Boonman, A. M. S., van Dishoeck, E. F., Lahuis, F., & Doty, S. D. 2003, A&A, 399, 1063

Collings, M. P., Dever, J. W., Fraser, H. J., & McCoustra, M. R. S. 2003a, Ap&SS, 285, 633

Collings, M. P., Dever, J. W., Fraser, H. J., McCoustra, M. R. S., & Williams, D. A. 2003b, ApJ, 583, 1058

Decius, J. C., & Hexter, R. M. 1977, Molecular Vibrations in Crystals (McGraw-Hill)

Ehrenfreund, P., Boogert, A. C. A., Gerakines, P. A., et al. 1996, A&A, 315, L341

Ehrenfreund, P., Boogert, A. C. A., Gerakines, P. A., Tielens, A. G. G. M., & van Dishoeck, E. F. 1997, A&A, 328, 649

Ehrenfreund, P., Kerkhof, O., Schutte, W. A., et al. 1999, A&A, 350, 240

Elsila, J., Allamandola, L. J., & Sandford, S. A. 1997, ApJ, 479, 818

Falck, M. 1986, J. Chem. Phys., 86, 560

Fraser, H. J., Collings, M. P., Dever, J. W., & McCoustra, M. R. S. 2004, MNRAS, 353, 59

Gerakines, P. A., Schutte, W. A., Greenberg, J. M., & van Dishoeck, E. F. 1995, A&A, 296, 810

Gerakines, P. A., Whittet, D. C. B., Ehrenfreund, P., et al. 1999, ApJ, 522, 357

Gibb, E. L., Whittet, D. C. B., Boogert, A. C. A., & Tielens, A. G. G. M. 2004, ApJS, 151, 35

Nummelin, A., Whittet, D. C. B., Gibb, E. L., Gerakines, P. A., & Chiar, J. E. 2001, ApJ, 558, 185

Pontoppidan, K. M., Fraser, H. J., Dartois, E., et al. 2003, A&A, 408, 981

Pontoppidan, K. M., Dullemond, C. P., van Dishoeck, E. F., et al. 2005, ApJ, 622, 463

Roser, J. E., Vidali, G., Manicò, G., & Pirronello, V. 2001, ApJ, 555, L61

Sandford, S. A., & Allamandola, L. J. 1990, ApJ, 355, 357

Sandford, S. A., Allamandola, L. J., Tielens, A. G. G. M., & Valero, G. J. 1988, ApJ, 329, 498

van Dishoeck, E. F., Helmich, F. P., de Graauw, T., et al. 1996, A&A, 315, L349

Watanabe, N., & Kouchi, A. 2002, ApJ, 567, 651

Watson, D. M., Kemper, F., Calvet, N., et al. 2004, ApJS, 154, 391

Whittet, D. C. B., Gerakines, P. A., Tielens, A. G. G. M., et al. 1998, ApJ, 498, L159